Spin-density wave in the vicinity of superconducting state in λ-$(BETS)_2GaBr_xCl_{4-x}$ probed by ^{13}C NMR spectroscopy

T. Kobayashi [1,*] T. Ishikawa,[2] A. Ohnuma,[2] M. Sawada,[2] N. Matsunaga,[2] H. Uehara,[2] and A. Kawamoto [2]

[1]*Graduate School of Science and Engineering, Saitama University, Saitama 338-8570, Japan*

[2]*Department of Condensed Matter Physics, Graduate School of Science, Hokkaido University, Sapporo 060-0810, Japan*

(Received 14 January 2020; revised manuscript received 27 February 2020; accepted 10 March 2020; published 24 April 2020)

^{13}C NMR and electrical resistivity of λ-$(BETS)_2GaBr_{0.75}Cl_{3.25}$ [BETS: bis(ethylenedithio) tetraselenafulvalene] were simultaneously measured to clarify the electronic state of the insulating phase near the boundary of the superconducting (SC) phase of λ-$(BETS)_2GaCl_4$. We found the divergent peak in the nuclear spin-lattice relaxation rate divided by temperature $1/T_1T$ with the metal-insulator transition at 13 K, below which the appearance of internal fields in NMR spectra was confirmed. Results of this study indicate that λ-$(BETS)_2GaBr_{0.75}Cl_{3.25}$ undergoes spin-density-wave (SDW) ordering. We suggest that the existence of the SDW phase in the vicinity of the SC phase can explain the unexplainable enhancement of $1/T_1T$ at low temperatures observed in λ-$(BETS)_2GaCl_4$, and SDW fluctuation plays an important role in the pairing mechanism of λ-type BETS superconductors.

DOI: 10.1103/PhysRevResearch.2.023075

The effect of electronic correlation on superconductivity is a central issue in the field of condensed matter physics. Thus far, organic conductors have considerably contributed to this field by providing valuable information, because the superconducting (SC) phase appears near the magnetic or charge-ordering insulating phase due to the competition between the Coulomb interaction and bandwidth [1]. Moreover, these electronic phases can systematically be tuned using chemical substitution and external pressure. Charge-transfer salts $(TMTCF)_2X$ (C = S; TMTTF: tetramethyltetrathiafulvalene, C = Se; TMTSF: tetramethyltetraselenafulvalene) and κ-$(ET)_2X$ [ET: bis(ethylenedithio)tetrathiafulvalene] are representative organic superconductors whose general phase diagrams have been extensively studied, where X is a monovalent anion. $(TMTCF)_2X$ shows the SC phase neighboring the spin-density-wave (SDW) phase [2,3], whereas in κ-$(ET)_2X$, the SC phase is adjacent to the antiferromagnetic (AF) Mott insulating phase [4]. Experimental studies have demonstrated different electronic properties depending on adjacent phases; that is, κ-$(ET)_2X$ and $(TMTCF)_2X$ exhibit Fermi-liquid and non-Fermi-liquid behavior just above the SC transition, respectively [5–8]. Theoretically, the interplay between superconductivity and magnetism is also discussed [9–12]. Thus, understanding the adjacent insulating phase is key to revealing the mechanism of unconventional superconductivity.

Quasi-two-dimensional organic conductors λ-$(BETS)_2MCl_4$ [BETS: bis(ethylenedithio)tetraselenafulvalene, M = Ga, Fe] also have rich topics alongside the systems of $(TMTCF)_2X$ and κ-$(ET)_2X$. Novel SC phenomena have been proposed in λ-$(BETS)_2GaCl_4$, such as d-wave SC gap symmetry [13,14] and Fulde-Ferrell-Larkin-Ovchinnikov (FFLO) states near the upper critical field [15–17]. The isostructural λ-$(BETS)_2FeCl_4$ shows the field-induced superconductivity at 17–42 T below 1 K [18,19], where the FFLO phases are adjacent to sandwich the SC phase [20]. A study on λ-$(BETS)_2Fe_xGa_{1-x}Cl_4$ demonstrated that the magnetic fields where the field-induced SC phase appears decrease with the iron ion continuously [21], indicating that the SC mechanism of both salts is equivalent. To understand the SC mechanism of λ-type salts, a study on λ-$(BETS)_2GaCl_4$ is primarily required; however, the general phase diagram and properties of the adjacent insulating phase have not been established.

In the study on λ-D_2GaCl_4 (donor molecules: D = ET, STF, BETS), a pressure–temperature (P–T) phase diagram was proposed with variations in the bandwidth, which was achieved by substituting the donor molecules with each other [22–24]. In this phase diagram, the SC and AF Mott insulating phases stand apart because there is a paramagnetic insulating phase between the two phases. Meanwhile, Kobayashi *et al.* investigated the adjacent insulating phase using the negative chemical pressure effect by substituting the anion in the series of λ-$(BETS)_2GaBr_xCl_{4-x}$ [25,26]. The temperature dependence of the resistivity of the sample at $x \sim 0.7$, which is in close proximity to the SC phase, exhibits an unexplainable semiconductor-metal-insulator behavior with decreasing temperature. At $x > 1$, the resistivity exhibits semiconducting behavior in the whole temperature range. Despite these different electrical properties, the electronic properties of these samples

*tkobayashi@phy.saitama-u.ac.jp

are believed to be the same in a nonmagnetic insulating (NMI) state [26]. Thus, the detailed nature of this phase is unknown. More interestingly, the increase in the spin-lattice relaxation rate divided by temperature $1/T_1T$ below 10 K was observed by ^{13}C nuclear magnetic resonance (NMR) measurement for λ-$(BETS)_2GaCl_4$ [27]. This behavior is considered to be due to the spin fluctuation originating from the adjacent insulating phase; however, the exact details are still being discussed. To elucidate the aforementioned problems, an understanding of electronic and magnetic properties in the insulating phase of λ-type salt is required.

For investigating the magnetic properties, NMR spectroscopy is a powerful technique which has several advantages over other techniques, including its ability to observe magnetic fluctuations from the spin-lattice relaxation time T_1 and the magnetic transition directly from the NMR spectrum. In this study, we measured ^{13}C NMR in conjunction with the resistivity for λ-$(BETS)_2GaBr_{0.75}Cl_{3.25}$, which is located near the boundary between the SC and the NMI phases, to examine the electric and magnetic properties simultaneously.

Single crystals of λ-$(BETS)_2GaBr_{0.75}Cl_{3.25}$ were prepared by electrochemical oxidation [26]. For ^{13}C NMR measurement, we used ^{13}C-enriched BETS molecules in which one side of the central C=C bond was enriched in accordance with the literature [27]. The sample size for the resistivity measurement is $1.1 \times 0.23 \times 0.12$ mm^3. The electrical resistivity was measured in the range from 300 to 4 K by the four-probe method with the electric current along the thin needle axis of the crystal (c axis). Gold wires ($\phi 10$ μm) were attached to the sample using carbon paste. The size of a single crystal used for ^{13}C NMR measurement is $8.0 \times 0.23 \times 0.12$ mm^3. ^{13}C NMR was measured under a magnetic field of 6 T. The field direction of the sample was rotated around the c axis. The orientation of the magnetic field θ was measured from the magnetic field parallel to the conduction plane. The spectra were obtained by fast Fourier transformation of an echo signal with a $\pi/2$-π pulse sequence. A $\pi/2$ pulse width is 4 and 1.5 μs for the measurement at $\theta = 72^\circ$ and -18°, respectively. Tetramethylsilane (TMS) was adopted as the reference material of the NMR shift. T_1 was measured using a conventional saturation-recovery method. Note that the same single crystal was used for both resistivity and ^{13}C NMR measurements, which enables us to discuss the electric and magnetic properties without sample dependence.

Figure 1 shows the temperature dependence of resistivity of λ-$(BETS)_2GaBr_{0.75}Cl_{3.25}$ (solid blue line with right scale). The resistivity is normalized by its room-temperature resistivity value. With a decrease in temperature, the resistivity varies from a semiconducting to a metallic behavior passing through a broad maximum at 30 K, indicating the crossover. At 15 K, the resistivity exhibits clear metal-insulator (MI) transition. These behaviors are consistent with the previous result of λ-$(BETS)_2GaBr_{0.75}Cl_{3.25}$ [26]. The present result represents that our sample indeed stands adjacent to the SC phase in the P–T phase diagram.

The T_1 measurement provides information regarding the spin fluctuation that is crucial for deep understanding of the magnetic properties. The temperature dependence of $1/T_1T$ of λ-$(BETS)_2GaBr_{0.75}Cl_{3.25}$ and λ-$(BETS)_2GaCl_4$ [27] is represented along the left axis, as shown in Fig. 1. T_1 measurement

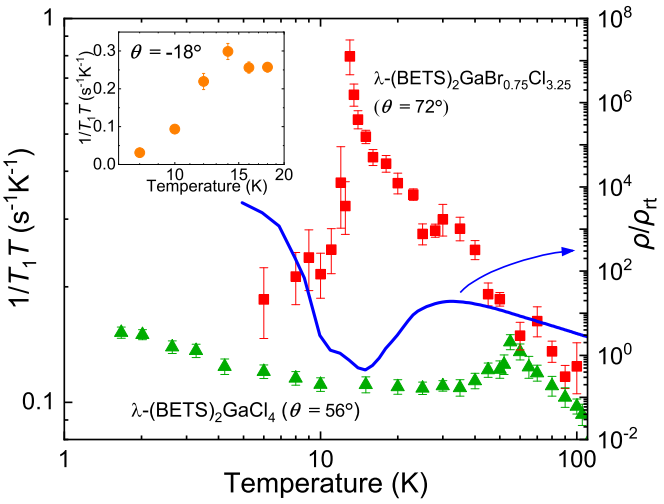

FIG. 1. Temperature dependence of $1/T_1T$ of λ-$(BETS)_2GaBr_{0.75}Cl_{3.25}$ and λ-$(BETS)_2GaCl_4$ (left scale) and that of the resistivity of λ-$(BETS)_2GaBr_{0.75}Cl_{3.25}$ (right scale). The inset shows the temperature dependence of $1/T_1T$ of λ-$(BETS)_2GaBr_{0.75}Cl_{3.25}$ measured at $\theta = -18^\circ$.

of λ-$(BETS)_2GaBr_{0.75}Cl_{3.25}$ was conducted at $\theta = 72^\circ$ to obtain the shortest T_1 that improves the signal-to-noise ratio of signals at a short repetition time. At high temperatures, $1/T_1T$ of λ-$(BETS)_2GaBr_{0.75}Cl_{3.25}$ increases with decreasing temperature and shows a kink at approximately 30 K, where the resistivity shows the crossover from semiconductor to metal. Similar behavior was observed in λ-$(BETS)_2GaCl_4$, in which $1/T_1T$ shows a sharp peak at 55 K with the semiconductor-metal crossover characterized by the inflection point of the resistivity [27]. Such a relation between the resistivity and $1/T_1T$ is observed in a κ-type superconductor that is situated close to the Mott AF phase [5,28,29]. Considering these results and similar intermolecular overlap integrals between λ-$(BETS)_2GaCl_4$ and κ-$(ET)_2Cu[N(CN)_2]Br$ [26,30], the AF fluctuation at high temperatures in λ-type salt originates from the AF Mott insulating phase. In fact, the isostructural λ-$(ET)_2GaCl_4$ shows the AF dimer-Mott insulating phase revealed by ^{13}C NMR study [24].

Below the crossover temperature in the metallic state, λ-$(BETS)_2GaCl_4$ shows the Fermi-liquid behavior characterized by the temperature-independent $1/T_1T$ [27]. However, $1/T_1T$ of λ-$(BETS)_2GaBr_{0.75}Cl_{3.25}$ increases again below 25 K and diverges at 13 K, while the resistivity exhibits MI transition. Different from the AF transition in the Mott insulator, these results indicate that the magnetic transition is accompanied by a MI transition. Indeed, the spin susceptibility of λ-$(BETS)_2GaBr_{0.7}Cl_{3.3}$ for a powder sample shows a slight decrease below 15 K [25].

To clarify the mechanism of spin fluctuation below 25 K, the NMR spectrum provides significant information for magnetic transition. Figure 2(a) shows the ^{13}C NMR spectra at several temperatures at $\theta = 72^\circ$. In λ-$(BETS)_2GaBr_{0.75}Cl_{3.25}$, which has almost the same crystal structure as λ-$(BETS)_2GaCl_4$ [26], there are two crystallographically nonequivalent BETS molecules in a unit cell, and each molecule has two nonequivalent ^{13}C sites, resulting in

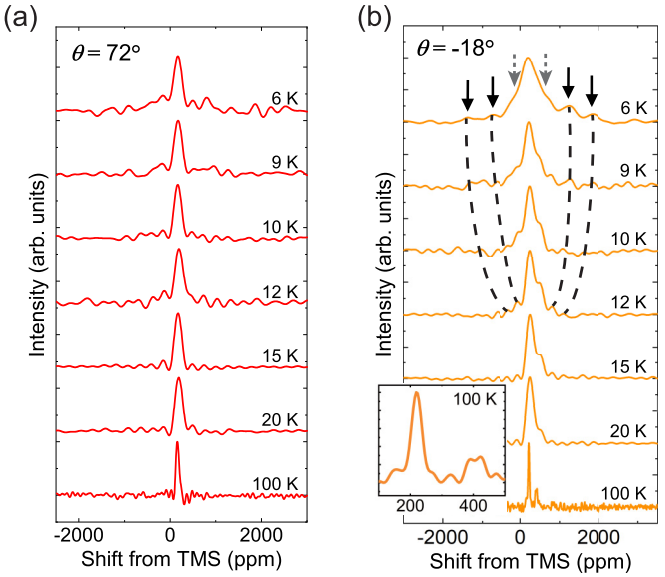

FIG. 2. Temperature evolution of NMR spectra of the λ-$(BETS)_2GaBr_{0.75}Cl_{3.25}$ at (a) $\theta = 72°$ and (b) $\theta = -18°$. The arrows at 6 K indicate discrete peaks due to the appearance of the internal field. Dashed lines are guides to the eye.

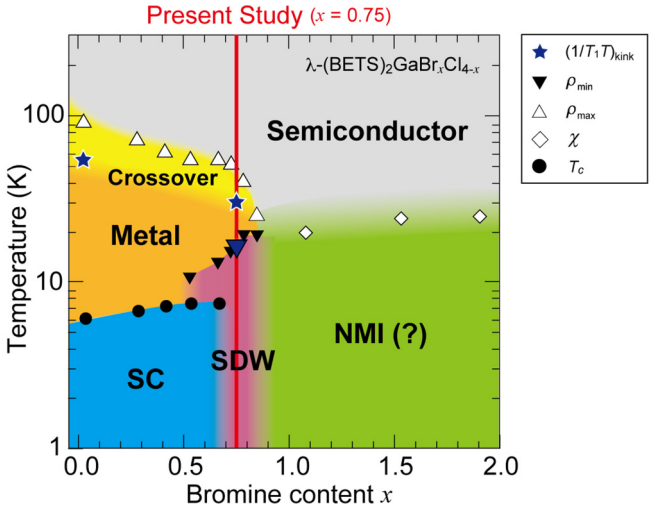

FIG. 3. Phase diagram of λ-$(BETS)_2GaBr_xCl_{4-x}$ as a function of bromine content x [26]. $(1/T_1T)_{kink}$, ρ_{min}, ρ_{max}, χ, and T_c are defined by the temperatures exhibiting the $1/T_1T$ maximum, metal-insulator transition, broad resistivity maximum, considerable decrease in spin susceptibility, and SC transition, respectively.

four independent peaks. At 100 K, the four sites are merged as they have nearly the same hyperfine coupling constant; hence, there is one sharp peak at approximately 160 ppm. Although $1/T_1T$ diverges at 13 K, the peak becomes slightly broadened, and the peak position barely changes with decreasing temperature, implying that the magnitude of the internal field is small.

For a more detailed spectrum study, we searched for an angle where the shift would change significantly and measured the temperature evolution of the NMR spectrum at $\theta = -18°$, as shown in Fig. 2(b). At 100 K, two sharp peaks were observed at 219 and 429 ppm which are consistent with the NMR spectra of λ-$(BETS)_2GaCl_4$ [27]. Judging from the intensity ratio between two peaks as discussed in Ref. [27], three sites are merged into a low-frequency peak owing to nearly the same hyperfine coupling constant. Below 20 K, two peaks are superposed, and the linewidth increases on further cooling. The asymmetrical spectra change symmetrically around the chemical shift position at 6 K. The spectra have a shoulder structure (marked by dotted arrows) in the center peak with several additional symmetrical discrete peaks (solid arrows). To verify whether the center broad peak below 13 K originates from the magnetically ordered or metallic part of the sample, we measured $1/T_1T$ at $\theta = -18°$ as shown in the inset of Fig. 1. $1/T_1T$ shows a peak behavior at 14 K and drastically decreases down to 8 K. This behavior is consistent with the result at $\theta = 72°$; therefore, we conclude that the center peak originates from the magnetic ordering state. These results suggest the development of multiple internal fields with different magnitudes, which cannot be understood by a simple up-down magnetic structure.

The present NMR results of diverging in $1/T_1T$ and the existence of several discrete NMR peaks, including the center peak with small internal field, were similarly observed in the ^{13}C NMR study of $(TMTTF)_2Br$ [31,32], which undergoes a commensurate SDW transition below 13 K [33,34]. In the commensurate SDW, distinctly separated spectra were observed, while in the incommensurate SDW represented by $(TMTSF)_2PF_6$ [35], a characteristic U-shaped spectrum was observed. In λ-$(BETS)_2GaBr_{0.75}Cl_{3.25}$, although the precise magnetic structure cannot be determined due to limited spectral resolution, the spectral shape was observed to be close to that expected in the commensurate SDW. In addition, $1/T_1$ of $(TMTTF)_2Br$ demonstrated temperature dependence of the thermal activation type in the commensurate SDW state [31,32], whereas $1/T_1$ of $(TMTSF)_2PF_6$ followed the power-law behavior below the transition to the incommensurate SDW state [35]. The drastic decrease in $1/T_1T$ below 13 K in λ-$(BETS)_2GaBr_{0.75}Cl_{3.25}$ is similar to the behavior of $(TMTTF)_2Br$, suggesting that λ-$(BETS)_2GaBr_{0.75}Cl_{3.25}$ exhibits the commensurate SDW state.

The manifestation of an SDW state requires the nesting instability of the Fermi surface. In λ-type salt, this effect is expected because the Fermi surface comprises a closed pocket and two sheets of the Fermi surfaces with flat parts [36,37]. In addition, λ-$(BETS)_2GaCl_4$ and λ-$(BETS)_2FeCl_4$ show the FFLO state [15–17,20], the stability of which is intimately related to the nesting condition of the Fermi surface [38].

The result that the SDW phase is adjacent to the SC phase of λ-$(BETS)_2GaCl_4$ modifies the P–T phase diagram of λ-$(BETS)_2GaBr_xCl_{4-x}$ determined by the resistivity and spin susceptibility measurements, as shown in Fig. 3 [26]. This SDW phase certainly affects the electronic properties of λ-$(BETS)_2GaCl_4$ because $1/T_1T$ of λ-$(BETS)_2GaCl_4$ increases below 10 K when the superconductivity is suppressed by the magnetic field [27]. Similar behavior was observed in $(TMTSF)_2PF_6$, which exhibits SDW ordering at ambient pressure and superconductivity under pressures. $1/T_1T$ shows Curie-Weiss behavior due to SDW ordering at ambient pressure. Applying pressure suppresses the enhancement of $1/T_1T$ at low temperature; however, Curie-Weiss behavior

indicating SDW fluctuation still remains until superconductivity disappears [8]. Resistivity also exhibits non-Fermi-liquid behavior at the corresponding pressures [7]. Applying pressure in $(TMTSF)_2PF_6$ corresponds to the decrease in the bromine content in λ-$(BETS)_2GaBr_xCl_{4-x}$. As discussed in $(TMTSF)_2X$ [11], SDW fluctuation is suggested to play an important role in the occurrence of superconductivity in λ-$(BETS)_2GaCl_4$. In fact, Fermi surface nesting has been considered to discuss the SC gap function theoretically in λ-$(BETS)_2GaCl_4$ [39].

The discovery of SDW ordering in λ-$(BETS)_2GaBr_xCl_{4-x}$ might unravel the mysterious AF ordering with MI transition in λ-$(BETS)_2FeCl_4$. It is uncertain whether the AF ordering originates from the Fe 3*d* spins or π spins of the BETS molecules, which is triggered by the observation of excess specific heat below 8 K, indicating the paramagnetic spin state of Fe 3*d* spins even in the AF state [40,41]. Considering that the isostructural λ-$(BETS)_2GaCl_4$ is a superconductor with SDW fluctuations, Fe 3*d* spins may stabilize the SDW state in λ-$(BETS)_2FeCl_4$.

λ-$(BETS)_2GaBr_{0.75}Cl_{3.25}$ shows the SDW ordering with MI transition; however, when x increases in λ-$(BETS)_2GaBr_xCl_{4-x}$, the system exhibits semiconducting behavior in all temperature ranges and shows a decrease in the spin susceptibility below 30 K without anisotropy [26]. These results indicate that the electronic properties are evidently different between $x \sim 0.7$ and $x > 1.0$ (Fig. 3). However, more detailed studies have not been conducted on the NMI phase, including even whether the phase is really nonmagnetic. Therefore, further investigation is required to obtain a better understanding of the λ-$(BETS)_2GaBr_xCl_{4-x}$ system.

In summary, to investigate the nature of the insulating phase that is adjacent to the SC phase of λ-$(BETS)_2GaCl_4$, we measured the ^{13}C NMR and resistivity of λ-$(BETS)_2GaBr_{0.75}Cl_{3.25}$. An increase in the $1/T_1T$ upon cooling is exhibited in the semiconducting state, indicating the development of the AF fluctuation due to the AF Mott insulating phase. With the crossover from semiconductor to metal, $1/T_1T$ shows a kink and increases again toward 13 K even in the metallic state. Considering the divergence of $1/T_1T$ at 13 K and the split into several peaks symmetrically in the NMR spectrum, λ-$(BETS)_2GaBr_{0.75}Cl_{3.25}$ exhibits the SDW ordering. These results suggest that the increase in $1/T_1T$ just above the SC transition in λ-$(BETS)_2GaCl_4$ originates from the SDW fluctuation, which should be considered as a pairing mechanism of superconductivity.

This work was partly supported by Hokkaido University, Global Facility Center (GFC), Advanced Physical Property Open Unit (APPOU), funded by MEXT under "Support Program for Implementation of New Equipment Sharing System" (JPMXS0420100318). It was also partially supported by the Japan Society for the Promotion of Science KAKENHI Grants No. 16J06398, No. 18H05843, and No. 16K05427.

[1] A. Ardavan, S. Brown, S. Kagoshima, K. Kanoda, K. Kuroki, M. Hatsumi, M. Ogata, S. Uji, J. Wosnitza, A. Ardavan, S. Brown, S. Kagoshima, K. Kanoda, K. Kuroki, H. Mori, M. Ogata, S. Uji, and J. Wosnitza, J. Phys. Soc. Jpn. **81**, 011004 (2012).
[2] D. Jérome and H. Schulz, Adv. Phys. **31**, 299 (1982).
[3] D. Jérome, Science **252**, 1509 (1991).
[4] K. Kanoda, Hyperfine Interact. **104**, 235 (1997).
[5] C. Strack, C. Akinci, V. Paschenko, B. Wolf, E. Uhrig, W. Assmus, M. Lang, J. Schreuer, L. Wiehl, J. A. Schlueter, J. Wosnitza, D. Schweitzer, J. Müller, and J. Wykhoff, Phys. Rev. B **72**, 054511 (2005).
[6] M. Itaya, Y. Eto, A. Kawamoto, and H. Taniguchi, Phys. Rev. Lett. **102**, 227003 (2009).
[7] N. Doiron-Leyraud, P. Auban-Senzier, S. René de Cotret, C. Bourbonnais, D. Jérome, K. Bechgaard, and L. Taillefer, Phys. Rev. B **80**, 214531 (2009).
[8] Y. Kimura, M. Misawa, and A. Kawamoto, Phys. Rev. B **84**, 045123 (2011).
[9] J. Schmalian, Phys. Rev. Lett. **81**, 4232 (1998).
[10] H. Kino and H. Kontani, J. Phys. Soc. Jpn. **67**, 3691 (1998).
[11] C. Bourbonnais and A. Sedeki, Phys. Rev. B **80**, 085105 (2009).
[12] J. C. Nickel, R. Duprat, C. Bourbonnais, and N. Dupuis, Phys. Rev. B **73**, 165126 (2006).
[13] S. Imajo, N. Kanda, S. Yamashita, H. Akutsu, Y. Nakazawa, H. Kumagai, T. Kobayashi, and A. Kawamoto, J. Phys. Soc. Jpn. **85**, 043705 (2016).
[14] S. Imajo, S. Yamashita, H. Akutsu, H. Kumagai, T. Kobayashi, A. Kawamoto, and Y. Nakazawa, J. Phys. Soc. Jpn. **88**, 023702 (2019).
[15] M. A.Tanatar, T. Ishiguro, H. Tanaka, and H. Kobayashi, Phys. Rev. B **66**, 134503 (2002).
[16] W. A. Coniglio, L. E. Winter, K. Cho, C. C. Agosta, B. Fravel, and L. K. Montgomery, Phys. Rev. B **83**, 224507 (2011).
[17] S. Uji, K. Kodama, K. Sugii, T. Terashima, T. Yamaguchi, N. Kurita, S. Tsuchiya, T. Konoike, M. Kimata, A. Kobayashi, B. Zhou, and H. Kobayashi, J. Phys. Soc. Jpn. **84**, 104709 (2015).
[18] S. Uji, H. Shinagawa, T. Terashima, T. Yakabe, Y. Terai, M. Tokumoto, A. Kobayashi, H. Tanaka, and H. Kobayashi, Nature (London) **410**, 908 (2001).
[19] L. Balicas, J. S. Brooks, K. Storr, S. Uji, M. Tokumoto, H. Tanaka, H. Kobayashi, A. Kobayashi, V. Barzykin, and L. P. Gor'kov, Phys. Rev. Lett. **87**, 067002 (2001).
[20] S. Uji, T. Terashima, M. Nishimura, Y. Takahide, T. Konoike, K. Enomoto, H. Cui, H. Kobayashi, A. Kobayashi, H. Tanaka, M. Tokumoto, E. S. Choi, T. Tokumoto, D. Graf, and J. S. Brooks, Phys. Rev. Lett. **97**, 157001 (2006).
[21] S. Uji, T. Terashima, C. Terakura, T. Yakabe, Y. Terai, S. Yasuzuka, Y. Imanaka, M. Tokumoto, A. Kobayashi, F. Sakai, H. Tanaka, H. Kobayashi, L. Balicas, and J. S. Brooks, J. Phys. Soc. Jpn. **72**, 369 (2003).
[22] H. Mori, T. Okano, M. Kamiya, M. Haemori, H. Suzuki, S. Tanaka, Y. Nishio, K. Kajita, and H. Moriyama, Physica C **357–360**, 103 (2001).

[23] T. Minamidate, Y. Oka, H. Shindo, T. Yamazaki, N. Matsunaga, K. Nomura, and A. Kawamoto, J. Phys. Soc. Jpn. **84**, 063704 (2015).
[24] Y. Saito, S. Fukuoka, T. Kobayashi, A. Kawamoto, and H. Mori, J. Phys. Soc. Jpn. **87**, 013707 (2018).
[25] H. Kobayashi, H. Akutsu, E. Arai, H. Tanaka, and A. Kobayashi, Phys. Rev. B **56**, R8526 (1997).
[26] H. Tanaka, A. Kobayashi, A. Sato, H. Akutsu, and H. Kobayashi, J. Am. Chem. Soc. **121**, 760 (1999).
[27] T. Kobayashi and A. Kawamoto, Phys. Rev. B **96**, 125115 (2017).
[28] A. Kawamoto, K. Miyagawa, Y. Nakazawa, and K. Kanoda, Phys. Rev. Lett. **74**, 3455 (1995).
[29] Y. Kurosaki, Y. Shimizu, K. Miyagawa, K. Kanoda, and G. Saito, Phys. Rev. Lett. **95**, 177001 (2005).
[30] T. Mori, H. Mori, and S. Tanaka, Bull. Chem. Soc. Jpn. **72**, 179 (1999).
[31] E. Barthel, G. Quirion, P. Wzietek, D. Jérome, J. B. Christensen, M. Jørgensen, and K. Bechgaard, Europhys. Lett. (EPL) **21**, 87 (1993).
[32] S. Hirose, Y. Liu, and A. Kawamoto, Phys. Rev. B **88**, 125121 (2013).
[33] F. Creuzet, T. Takahashi, D. Jérome, and J. Fabre, J. Phys. Lett. **43**, 755 (1982).
[34] S. S. P. Parkin, J. C. Scott, J. B. Torrance, and E. M. Engler, Phys. Rev. B **26**, 6319 (1982).
[35] S. Nagata, M. Misawa, Y. Ihara, and A. Kawamoto, Phys. Rev. Lett. **110**, 167001 (2013).
[36] H. Kobayashi, H. Tomita, T. Naito, A. Kobayashi, F. Sakai, T. Watanabe, and P. Cassoux, J. Am. Chem. Soc. **118**, 368 (1996).
[37] C. Mielke, J. Singleton, M.-S. Nam, N. Harrison, C. C. Agosta, B. Fravel, and L. K. Montgomery, J. Phys.: Condens. Matter **13**, 8325 (2001).
[38] H. Shimahara, Phys. Rev. B **50**, 12760 (1994).
[39] H. Aizawa, T. Koretsune, K. Kuroki, and H. Seo, J. Phys. Soc. Jpn. **87**, 093701 (2018).
[40] H. Akiba, S. Nakano, Y. Nishio, K. Kajita, B. Zhou, A. Kobayashi, and H. Kobayashi, J. Phys. Soc. Jpn. **78**, 033601 (2009).
[41] Y. Oshima, H. Cui, and R. Kato, Magnetochemistry **3**, 10 (2017).